

Transport and relaxation in degenerate quark plasmas

H. Heiselberg

*Niels Bohr Institute, Blegdamsvej 17, DK-2100 Copenhagen Ø, Denmark
and Nuclear Science Division, MS 70A-3307, Lawrence Berkeley Laboratory, Berkeley, California 94720*

C. J. Pethick

*NORDITA, Blegdamsvej 17, DK-2100 Copenhagen Ø, Denmark
and Department of Physics, University of Illinois at Urbana-Champaign,
1110 West Green Street, Urbana, Illinois 61801-3080*

(Received 4 March 1993)

Transport coefficients and relaxation times are calculated for degenerate quark matter within perturbative QCD for temperatures T and inverse screening lengths q_D much smaller than the quark chemical potentials. The important physical effect is “dynamical screening” of transverse interactions. The physics changes significantly when $T \sim q_D$ and all relaxation times change from a power law dependence on T for $T \ll q_D$ to a power law times a logarithmic one for $T \gg q_D$. Results differ very much from standard Fermi liquid results in both limits. Detailed analytical calculations of the momentum relaxation time for interpenetrating quark plasmas, the diffusion coefficient, electrical conductivity, viscosity, and the thermal conductivity are performed to leading orders in the coupling constant. Applications to diffusion processes in the burning of neutron stars into strange quark matter and to electrical conduction in quark matter are given.

PACS number(s): 12.38.Bx, 12.38.Mh, 21.65.+f, 97.60.Jd

I. INTRODUCTION

Transport and relaxation properties of quark and gluon (QCD) plasmas are important in a number of different contexts. First they play a role in determining the time that it would take a quark-gluon plasma formed in a heavy-ion collision to approach equilibrium. Second, they are of interest in astrophysical situations such as the early Universe, and possibly neutron stars.

The basic difficulty in calculating transport properties of such plasmas, as well as of relativistic electron-photon (QED) plasmas, is the singular nature of the long-range interactions between constituents, which leads to divergences in scattering cross sections similar to those for Rutherford scattering. This makes the problem of fundamental methodological interest, in addition to its possible applications. The first approaches to describe the transport properties of quark-gluon plasmas employed the relaxation time approximation [1–3] for the collision term. This approximation simplifies the collision integral enormously and transport coefficients are related directly to the relaxation time. The latter is typically estimated from a characteristic cross section times the density of scatterers. In Refs. [2, 3] the divergent part of the total cross section at small momentum transfers was assumed to be screened at momentum transfers less than the Debye momentum. However, Debye screening influences only the longitudinal (electric) part of the QED and QCD interactions, and the transverse (magnetic) part is unscreened in the static limit.

Recently it has been shown that the physics responsible

for cutting off transverse interactions at small momenta is dynamical screening [4, 5]. This effect is due to Landau damping of the exchanged gluons or photons, and is analogous to the anomalous skin effect in pure metals [6]. Within perturbative QCD and QED rigorous analytical calculations of transport coefficients have been made for temperatures high compared with the chemical potentials of the constituents [4]. In this paper we investigate in detail degenerate quark plasmas for which the temperature is much lower than the quark chemical potentials, μ_q . Previously, the transport properties of such systems have been studied by Haensel and Jerzak [7], who assumed that transverse interactions were cut off at large distances in much the same way as longitudinal ones.

A major part of this paper is devoted to a detailed analytical calculation within perturbative QCD of momentum relaxation rates and their applications to transport processes in degenerate quark matter. Though almost no thermal gluons are present in degenerate quark matter when $T \ll \mu_q$, the calculations are more complicated than for the high-temperature case since there are three scales: T , μ_q , and the Debye wave number q_D (we shall use units such that $\hbar = c = k_B = 1$). In high-temperature plasmas the quark chemical potentials may be neglected and one has only two scales. The resulting transport coefficients we find are qualitatively different from those obtained when $T \gg \mu_q$, and, in addition, depend on the ratio T/q_D . We find that the effects of dynamical screening are more pronounced for the degenerate case than for the high-temperature one. In particular the temperature dependence of relaxation rates is not given by the standard result, $\sim T^2$, for a normal Fermi

liquid with short-range interactions.

We shall first describe in Sec. II the transport theory we use, namely the Boltzmann equation, and the screening of long-range quark-quark interactions. In Sec. III, we then evaluate the collision term for the process of interpenetrating quark plasmas and calculating the momentum loss and the relaxation time. In Sec. IV we apply the momentum relaxation time to calculate the diffusion coefficient, the electrical conductivity, and to estimate the stopping time in ultrarelativistic heavy ion collisions. The calculation of the thermal conductivity and the shear viscosity for quark matter is postponed to the end since these are considerably more complicated to evaluate. Finally, in Sec. V we give a summary.

$$\begin{aligned} \left(\frac{\partial}{\partial t} + \mathbf{v}_{\mathbf{p}_1} \cdot \nabla_{\mathbf{r}} + \mathbf{F} \cdot \nabla_{\mathbf{p}_1} \right) f_q(\varepsilon_{\mathbf{p}}) &= \left(\frac{\partial f_q}{\partial t} \right)_{\text{coll}} \\ &= -(2\pi)^4 \sum_{q'} \nu_{q'} \sum_{234} |M_{qq'}|^2 [f_1 f_2 (1-f_3)(1-f_4) - f_3 f_4 (1-f_1)(1-f_2)] \\ &\quad \times \delta(\mathbf{p}_1 + \mathbf{p}_2 - \mathbf{p}_3 - \mathbf{p}_4) \delta(\varepsilon_1 + \varepsilon_2 - \varepsilon_3 - \varepsilon_4). \end{aligned} \quad (1)$$

The collision integral on the right-hand side (RHS) is given by the rate of q quarks scattering in and out of the state with momentum \mathbf{p}_1 by scattering on q' quarks with momentum \mathbf{p}_2 (see also Fig. 1), and $M_{qq'}$ is the scattering matrix element.

Since here we are only interested in properties that are spin and color independent, it is convenient to work with the squared modulus of the matrix element summed over final spins and colors, and averaged over initial ones, $\langle |M|^2 \rangle$. Thus $\langle |M|^2 \rangle = \langle |\mathcal{M}|^2 \rangle / (16\varepsilon_1 \varepsilon_2 \varepsilon_3 \varepsilon_4)$, where $\langle |\mathcal{M}|^2 \rangle$ is the invariant matrix element for the scattering process $12 \rightarrow 34$ in Fig. 1, summed over final states and averaged over initial states. \mathbf{F} is the external force applied to the system and $\nu_q = 6$ is the spin and color statistical factor for the quark flavors q and q' . For notational convenience we have abbreviated $f_q(\varepsilon_i)$ by f_i .

B. Screening of quark interactions

The matrix element squared for the scattering process $12 \rightarrow 34$ in Fig. 1, summed over final states and averaged

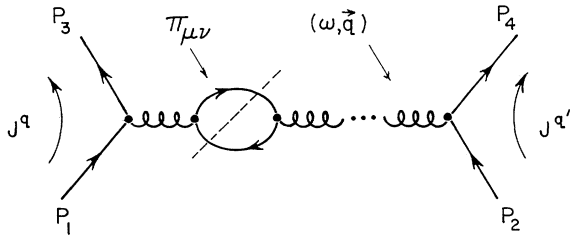


FIG. 1. Feynman diagram for quark-quark scattering including the gluon self-energy, Π , of which the leading order is just the $q\bar{q}$ bubble. Putting intermediate states in the bubble on the energy shell gives the imaginary part of Π^{RPA} due to absorption of the exchanged gluon by scattering on a quark (Landau damping).

II. TRANSPORT THEORY

A. Basic formalism

We shall in the following consider only situations where quantities vary slowly in space and time with respect to the typical scattering time, and the quark matter is assumed to be a weakly interacting gas of relativistic fermions. We describe the kinetics with the Boltzmann equation for the individual quark components. Since we work in the perturbative limit, we may neglect the effects of gluons on the dispersion relation for the quarks, as well as the Landau Fermi-liquid interactions among quasiparticles [8, 9]. The Boltzmann equation for the quark distribution function $f_q(\varepsilon_{\mathbf{p}})$ is thus simply

over initial states, is for scattering of quarks of different flavor [9]

$$\langle |M_{qq'}|^2 \rangle = \frac{4}{9} g^4 \frac{u^2 + s^2}{t^2}, \quad (2)$$

whereas for scattering of the same flavors of quarks

$$\langle |M_{qq}|^2 \rangle = \frac{4}{9} g^4 \left(\frac{s^2 + u^2}{t^2} + \frac{s^2 + t^2}{u^2} \right) - \frac{8}{27} \frac{s^2}{ut}. \quad (3)$$

These matrix elements are very singular because of the $t^{-2} = (\omega^2 - q^2)^{-2}$ dependence; here ω and \mathbf{q} are the energy and momentum transfer. The matrix element for scattering of like quarks is different due to the indistinguishability of final states; in particular there are now two singularities, u^{-2} and t^{-2} . However, because of this indistinguishability, the u and t channels are identical and we should divide by two to avoid double counting of final states. Therefore, there is no difference for small momentum transfers and the singular behavior that determines the transport processes for scattering of like quarks is the same as that of unlike quarks.

The bare QCD or QED interactions between two particles become screened in a plasma. The effects are taken into account by including the photon and gluon self-energies or polarization operator $\Pi_{\mu\nu}$ in the photon or gluon propagator $D_{\mu\nu}$. These are related by Dyson's equation

$$D_{\mu\nu}^{-1} = g_{\mu\nu}(\omega^2 - q^2) + \Pi_{\mu\nu}. \quad (4)$$

As shown by Weldon [10], the propagator splits into longitudinal and transverse parts with respect to \mathbf{q} with different polarization functions Π_l and Π_t respectively. The result is

$$\mathcal{M}_{qq'} = J_\mu^q D^{\mu\nu} J_\nu^{q'} = \frac{J_0^q J_0^{q'}}{q^2 + \Pi_l} - \frac{\mathbf{J}_t^q \cdot \mathbf{J}_t^{q'}}{q^2 - \omega^2 + \Pi_t}, \quad (5)$$

where J^q and $J^{q'}$ are the currents connected to the vertices involving q and q' , respectively (see Fig. 1). In (5) current conservation, $q^\mu J_\mu = \omega J_0 - q J_t = 0$, has been employed to relate the longitudinal ($J_l = \mathbf{J} \cdot \hat{\mathbf{q}}$) and timelike (J_0) components of the current.

In the random phase approximation the polarization functions (or self-energies) for photons or gluons are found by calculating the simple bubble diagrams of Fig. 1 [10, 11]. For small momentum transfers (the long wavelength limit), $q \ll \mu$, they are given by

$$\begin{aligned}\Pi_l &= q_D^2 \chi_l, \\ \Pi_t &= q_D^2 \chi_t,\end{aligned}\quad (6)$$

where

$$\begin{aligned}\chi_l &= \left[1 - \frac{x}{2} \ln \left(\frac{x+1}{x-1} \right) \right], \\ \chi_t &= \left[\frac{x^2}{2} + \frac{x(1-x^2)}{4} \ln \left(\frac{x+1}{x-1} \right) \right].\end{aligned}\quad (7)$$

[Note that our definition of Π_l differs from that of Weldon by a factor $(x^2 - 1)$.] Here $x = \omega/q$ and the Debye wave number for cold quark matter of N_q flavors is $q_D^2 = g^2 N_q \mu^2 / (2\pi^2)$.

We shall below repeatedly use the expansion close to the static limit, $x = \omega/q \simeq 0$, of the polarization functions:

$$\begin{aligned}\chi_l(x) &= 1 + O(x), \\ \chi_t(x) &= i\frac{\pi}{4}x + O(x^2),\end{aligned}\quad |x| \ll 1. \quad (8)$$

Note that the leading term in the transverse screening is imaginary. Both the longitudinal and transverse gluon self-energies have imaginary parts coming from Landau damping. Physically this corresponds to a virtual gluon being converted into a particle-hole pair. In other words, the intermediate state in the bubble diagram of Fig. 1 is on the energy shell.

To first order in the coupling constant the currents in (5) are given by $J_\mu^q = g\bar{u}(p_3)\gamma_\mu u(p_1)\lambda_\alpha^q/2$ and $J_\mu^{q'} = g\bar{u}(p_4)\gamma_\mu u(p_2)\lambda_\alpha^{q'}/2$ where u are Dirac spinors and λ_α are the usual Gell-Mann matrices connected to vertices q and q' . Because of the singular matrix element, the main contribution to $\mathbf{Q}_{qq'}$ will come from small momentum and energy transfers, i.e., $q \ll p_i \simeq \mu_q$. The magnetic moment contribution to the currents can then be neglected

(i.e., the spin does not flip in the small \mathbf{q} limit). The currents are then simply $J_\mu^q = g\lambda_\alpha^q p_{1,\mu}$ and $J_\mu^{q'} = g\lambda_\alpha^{q'} p_{2,\mu}$, and we find, from (5),

$$\mathcal{M}_{qq'} = \varepsilon_1 \varepsilon_3 g^2 \lambda_\alpha^q \lambda_\alpha^{q'} \left[\frac{1}{q^2 + \Pi_l} - \frac{\mathbf{v}_{1,t} \cdot \mathbf{v}_{2,t}}{q^2 - \omega^2 + \Pi_t} \right]. \quad (9)$$

Here, the massless particles travel with velocities $\mathbf{v}_i = \mathbf{p}_i/\varepsilon_i$ equal to the speed of light and $\mathbf{v}_{i,t}$ is the transverse component with respect to the direction of \mathbf{q} . For small \mathbf{q} , energy conservation implies that $\omega = \varepsilon_1 - \varepsilon_3 \simeq \mathbf{v}_1 \cdot \mathbf{q} = -\mathbf{v}_2 \cdot \mathbf{q}$. Therefore the velocity projections transverse to \mathbf{q} have lengths $|\mathbf{v}_{1,t}| = |\mathbf{v}_{2,t}| = \sqrt{1-x^2}$, and consequently $\mathbf{v}_{1,t} \cdot \mathbf{v}_{2,t} = (1-x^2)\cos\phi$, where ϕ is the angle between $\mathbf{v}_{1,t}$ and $\mathbf{v}_{2,t}$. The color degrees of freedom are included by taking the expectation values of the Gell-Mann matrices connected with each vertex: $|\lambda_\alpha^q \lambda_\alpha^{q'}|^2 = |\langle 3|\lambda_\alpha|1\rangle \langle 4|\lambda_\alpha|2\rangle|^2$. Summing over final-state colors is done by closure; since λ_α^2 is diagonal with trace 2, the averaging over initial states gives 4/9. Finally, summing over gluons, $\alpha = 1, \dots, 8$ gives us a resulting factor 32/9. From (9) we now obtain

$$\langle |M_{qq'}|^2 \rangle = \frac{2}{9} g^4 \left| \frac{1}{q^2 + \Pi_l} - \frac{(1-x^2)\cos\phi}{q^2 - \omega^2 + \Pi_t} \right|^2. \quad (10)$$

For massive quarks there would be additional factors of the particle velocities at the Fermi surface reducing the transverse or magnetic interaction [12]. For nonrelativistic systems such as laboratory metals the transverse part is therefore small, though it is important for some magnetic properties [6, 12, 13]. For relativistic particles, however, the transverse part is as important as the longitudinal one for hot plasmas whereas for cold degenerate plasmas we will show that in fact it is the dominant one.

III. MOMENTUM RELAXATION

The relevant quantity for transport processes such as momentum stopping, diffusion and electrical conductivity is the friction between the counterflowing quarks or equivalently the momentum transfer to quark flavors q due to collisions on all quark flavors q' . This is given by

$$\mathbf{Q}_q = \nu_q \sum_{\mathbf{p}_1} \mathbf{p}_1 \left(\frac{\partial f_q}{\partial t} \right)_{\text{coll}} \equiv \sum_{q'} \mathbf{Q}_{qq'}, \quad (11)$$

where the momentum transfer due to collisions between quarks of flavors q and q' is then given by (1):

$$\begin{aligned}\mathbf{Q}_{qq'} &= -(2\pi)^4 \nu_q \nu_{q'} \sum_{1234} \mathbf{p}_1 \langle |M_{qq'}|^2 \rangle [f_1 f_2 (1-f_3)(1-f_4) - f_3 f_4 (1-f_1)(1-f_2)] \\ &\quad \times \delta(\mathbf{p}_1 + \mathbf{p}_2 - \mathbf{p}_3 - \mathbf{p}_4) \delta(\varepsilon_1 + \varepsilon_2 - \varepsilon_3 - \varepsilon_4).\end{aligned}\quad (12)$$

If one uses the bare interactions, $\mathbf{Q}_{qq'}$ diverges because of the Rutherford-type singularity of QED and QCD interactions: $\langle |M_{qq'}|^2 \rangle \propto q^{-4}$. In transport processes this matrix element is usually weighted by $(1 - \cos\theta) \sim q^2$ and consequently $\mathbf{Q}_{qq'} \propto \int \langle |M_{qq'}|^2 \rangle q^3 dq$ will diverge logarithmically for small momentum transfer. This infrared divergence is cut off by Debye screening for the longitudinal interactions and by dynamical screening for the transverse interactions, as described in the previous section.

First we consider interpenetrating quark plasmas each in local equilibrium. The quark distribution functions are

$$f_q(\varepsilon_{\mathbf{p}}) = \{\exp[(\varepsilon_{\mathbf{p}} - \mu_q - \mathbf{u}_q \cdot \mathbf{p})/T_q] + 1\}^{-1}, \quad (13)$$

where $q = u, d, s, \dots$ refers to up quarks, down quarks, strange quarks, etc. Here the local temperature is denoted by T_q , the chemical potential by μ_q , and the flow velocity by \mathbf{u}_q , and all these quantities may depend on time and position in space. We shall investigate interpenetrating quark plasmas with different flow velocities but with a common temperature $T_q = T$. The distribution function of Eq. (13) is also the standard trial ansatz for calculating the diffusion coefficient and electrical conductivity which will be explored in Sec. V.

In (12) we can replace the factor \mathbf{p}_1 by $(\mathbf{p}_1 - \mathbf{p}_3)/2 = -\mathbf{q}/2$ due to symmetry. Furthermore, linearizing the distribution functions (13) in the flow velocities, one finds

$$f_i(\varepsilon_i) = f_i^0 - \frac{\partial f_i^0}{\partial \varepsilon_{\mathbf{p}}} \mathbf{u}_i \cdot \mathbf{p}, \quad (14)$$

where f^0 is the distribution function of Eq. (13) with $\mathbf{u} = 0$. The momentum transfer (12) is then given by

$$\mathbf{Q}_{qq'} = -(2\pi)^4 \nu_q \nu_{q'} \frac{\mathbf{u}_q - \mathbf{u}_{q'}}{6T} \sum_{1234} q^2 \langle |M_{qq'}|^2 \rangle f_1^0 f_2^0 (1 - f_3^0) (1 - f_4^0) \delta(\mathbf{p}_1 + \mathbf{p}_2 - \mathbf{p}_3 - \mathbf{p}_4) \delta(\varepsilon_1 + \varepsilon_2 - \varepsilon_3 - \varepsilon_4). \quad (15)$$

Introducing auxiliary integrals over the transferred momenta and energy (see Appendix A) the integrals over 1 and 3 separate from those over 2 and 4 and we find

$$\mathbf{Q}_{qq'} = -(2\pi)^4 \nu_q \nu_{q'} \frac{\mathbf{u}_q - \mathbf{u}_{q'}}{6T} \int_{-\infty}^{\infty} d\omega \int d^3 \mathbf{q} q^2 \langle |M_{qq'}|^2 \rangle S(\mu_q, q, \omega) S(\mu_{q'}, q, -\omega), \quad (16)$$

where the factor S is defined by

$$S(\mu_q, q, \omega) \equiv \sum_{\mathbf{p}_1, \mathbf{p}_3} f_q^0(p_1) [1 - f_q^0(p_3)] \delta(\mathbf{p}_1 - \mathbf{p}_3 - \mathbf{q}) \delta(p_1 - p_3 - \omega). \quad (17)$$

The quantity S is basically the dynamical structure factor of a free quark gas. It is evaluated in Appendix A in the limit of $\omega, T \ll \mu_q$ and is given by

$$S(\mu_q, q, \omega) = (2\pi)^{-5} \frac{\Theta(q - |\omega|)}{q} \mu_q^2 \Theta(2\mu_q - q) \frac{\omega}{1 - \exp(-\omega/T)}. \quad (18)$$

The cross term linear in $\cos \phi$ in the matrix element squared of (10) vanishes since there is no other dependence on ϕ and there will be an angular integration over ϕ (see Appendix A for details). The $\cos^2 \phi$ averages to 1/2. From (10), (16), and (18) we obtain, by changing variables from q to $x = \omega/q$,

$$\begin{aligned} \mathbf{Q}_{qq'} = & \frac{8}{3\pi^3} \alpha_s^2 T (\mathbf{u}_q - \mathbf{u}_{q'}) \mu_q^2 \mu_{q'}^2 \int_0^\infty \frac{d\omega}{\omega} \left(\frac{\omega/2T}{\sinh(\omega/2T)} \right)^2 \\ & \times \int_{|\omega|/2\mu_q}^1 dx \left[\frac{1}{|1 + (xq_D/\omega)^2 \chi_l(x)|^2} + \frac{1}{2} \frac{1}{|1 + (xq_D/\omega)^2 \chi_t(x)/(1-x^2)|^2} \right], \quad (19) \end{aligned}$$

where $\alpha_s = g^2/4\pi$ is the QCD fine structure constant.

Because the energy transfer is limited by the temperature, so that $|\omega| \lesssim T \ll \mu_q$, the lower limit on the x integration in (19) can be set to zero for the purpose of calculating the leading terms of order α_s^2 . In other words, large momentum transfers of order μ_q do not contribute to stopping. This is in contrast with the high-temperature plasma case where large momentum transfers of order T contribute to linear order, albeit not to the leading logarithmic order [4, 5]. We define the dimensionless integrals in (19) as

$$I_s(T/q_D) \equiv \int_0^\infty \frac{d\omega}{\omega} \left(\frac{\omega/2T}{\sinh(\omega/2T)} \right)^2 I_x(\omega), \quad (20)$$

$$I_x(\omega) \equiv \int_0^1 dx \left[\frac{1}{|1 + (xq_D/\omega)^2 \chi_l(x)|^2} + \frac{1}{2} \frac{1}{|1 + (xq_D/\omega)^2 \chi_t(x)/(1-x^2)|^2} \right]. \quad (21)$$

The integral in (20) cannot be evaluated analytically due to the complicated form of $\chi_{l,t}(x)$. The general features can, however, be extracted by evaluating it in limiting cases. For large energy transfers, $\omega \gg q_D$, screening does not affect the matrix element and the integral in

(21) is simply 3/2 (see Appendix B for more details), 1 from longitudinal interactions and 1/2 from transverse ones. For small energy transfers, $\omega \ll q_D$, the screening is essential in order to obtain a finite result. Since the major contribution to the integral (21) comes from small

values of x ($x \sim \omega/q_D$ or equivalently $q \sim q_D$), we can expand the $\chi_{l,t}(x)$ for small $x = \omega/q$ as given by (8). The integral over x in (21) becomes

$$I_x(\omega) = \int_0^1 dx \left[\frac{1}{[1 + (xq_D/\omega)^2]^2} + \frac{1}{2} \frac{1}{1 + (\pi/4)^2 (q_D/\omega)^4 x^6} \right], \quad |\omega| \ll q_D. \quad (22)$$

The upper limit can now be extended to ∞ and the integral is then straightforward to evaluate and so we obtain, for the two limits,

$$I_x(\omega) = \begin{cases} 3/2, & \omega \gg q_D, \\ \frac{\pi}{6} \left(\frac{4\omega^2}{\pi q_D^2} \right)^{1/3} + \frac{\pi\omega}{4q_D}, & \omega \ll q_D. \end{cases} \quad (23)$$

The two terms for $\omega \ll q_D$ correspond to the transverse and longitudinal interactions, respectively, and we note that the transverse part dominates in contrast with the $\omega \gg q_D$ limit where the transverse part is just half of the longitudinal part.

Next we perform the integration (20). When $T \gg q_D$, $I_s(T/q_D)$ is essentially an integral of $3/(2\omega)$ with a lower cutoff around q_D as seen in (23) and an upper cutoff around T as given by the Bose factors. Thus the leading term will be $\frac{3}{2} \ln(T/q_D)$ and the next order is a constant term evaluated in Appendix B. For the other case, $T \ll q_D$, the $\omega \ll q_D$ limit of (23) applies for I_x and is straightforward to evaluate. We find

$$I_s(T/q_D) = \begin{cases} \frac{3}{2} \ln(T/q_D) + 2.72, & T \gg q_D, \\ a \left(\frac{T}{q_D} \right)^{2/3} + \frac{\pi^3 T}{12 q_D}, & T \ll q_D, \end{cases} \quad (24)$$

where

$$a = \Gamma\left(\frac{8}{3}\right)\zeta\left(\frac{5}{3}\right)(2\pi)^{2/3}/6 \simeq 1.81. \quad (25)$$

In the limit $T \gg q_D$ the contribution to I_s from transverse interactions is just half that from longitudinal ones to leading logarithmic order. This follows from the fact that the contributions to I_s are in this ratio for $\omega \gg q_D$. In the limit $T \ll q_D$ the contribution to I_s from transverse interactions scales as $(T/q_D)^{2/3}$ and thus dominates the contributions from the longitudinal interactions, which scale as T/q_D as may be seen from (24). Employing the static limit (no transverse screening) would have led to a logarithmically diverging $I_s(T/q_D)$ since the lower limit would then have to be zero instead of $\sim q_D$. Thus we see the importance of the finite energy of the transferred gluon and the Landau damping during exchange (“dynamical screening”). $I_s(T/q_D)$ has been calculated numerically and the result is shown in Fig. 2. The analytical result (24) is quite good except in the region around $q_D \sim 2T$.

From (19) and (24) we finally obtain

$$\mathbf{Q}_{qq'} = -(\mathbf{u}_q - \mathbf{u}_{q'}) \mu_q^2 \mu_{q'}^2 \frac{8}{3\pi^3} T \alpha_s^2 I_s(T/q_D). \quad (26)$$

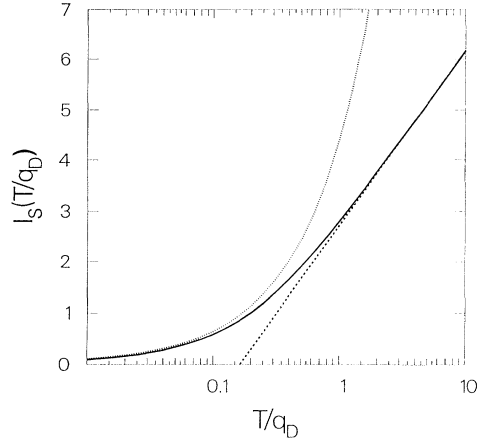


FIG. 2. The dimensionless function $I_s(T/q_D)$ given by (20). Dashed and dotted curves correspond to the $T \gg q_D$ and $T \ll q_D$ limits of $I_s(T/q_D)$, respectively, as given by (24).

Generally, $\mathbf{Q}_{qq'}$ is proportional to the relative flow velocities of the different quark flavors. The total momentum transfer, \mathbf{Q}_q , to quark flavors q by scattering on the other flavor q' can be written in the form

$$\mathbf{Q}_q \equiv \sum_{q'} \mathbf{Q}_{qq'} = -\frac{1}{\tau_s} \frac{1}{N_q} \sum_{q'} (\mathbf{u}_q - \mathbf{u}_{q'}) \frac{\mu_q^2 \mu_{q'}^2}{\pi^2}, \quad (27)$$

where the characteristic rate of momentum stopping by strong interactions, $1/\tau_s$, is, from (26) and (27),

$$\begin{aligned} \frac{1}{\tau_s} &= \frac{8N_q}{3\pi} T \alpha_s^2 I_s(T/q_D) \\ &= \frac{8N_q}{3\pi} \alpha_s^2 \times \begin{cases} \frac{3}{2} T \ln(T/q_D) + 2.72T, & T \gg q_D, \\ a \frac{T^{5/3}}{q_D^{2/3}} + \frac{\pi^3 T^2}{12 q_D}, & T \ll q_D. \end{cases} \end{aligned} \quad (28)$$

The physical significance of this time τ_s will be described further in the next section. Note that (27) satisfies the condition $\sum_q \mathbf{Q}_q = 0$ as required by conservation of total momentum.

The strong dependence on T/q_D in (28) arises because the stopping process is dominated by processes with small momentum transfers, $\sim q_D$. When $T \gg q_D$, (28) contains the usual logarithm of the maximum and minimum momentum transfer given by T and q_D , respectively [4, 5]. The screening of small momentum transfer $q \sim q_D$ is unaffected because the thermal smearing of the Fermi surface is greater than the inverse screening length. For $T \ll q_D$, however, we do not obtain the usual $\tau_s^{-1} \propto T^2$ result of Fermi liquid theory [14]; instead the leading term is $\tau_s^{-1} \propto T^{5/3}$ because Landau damping screens momentum transfers $q \lesssim (q_D^2 \omega)^{1/3}$, where the energy transfer ω is $\sim T$ [13].

The standard Fermi liquid result for a typical transport relaxation rate is that $1/\tau \propto T^2$. When $T \ll q_D$ this is actually what Eq. (28) gives for the longitudinal part of the interactions, because the longitudinal part of the matrix element, $\sim (q^2 + q_D^2)^{-2}$, is practically constant

for all energy transfers $\omega \lesssim T \ll q_D$. Consequently, the very singular interaction does not affect the temperature dependence for the longitudinal part when $T \ll q_D$ and we obtain the standard Fermi liquid result. However, for the transverse part or for $T \gg q_D$ the singular interactions give quite different temperature dependences as can be seen from (28). The same applies for the viscous and thermal relaxation rates, which we calculate below.

Let us now compare our results with those of Haensel and Jerzak [7]. They do not address the problem of transverse screening but implicitly assume that the transverse interactions, like the longitudinal ones, are screened for $q \lesssim q_D$. Second, they assume that $T \ll q_D$ so that their viscous and electrical relaxation rates are proportional to $\tau^{-1} \propto \alpha_s^2 T^2 / q_D \sim \alpha_s^{3/2} T^2$ which is also what one finds from (28) for $T \ll q_D$ when transverse interactions are ignored. However, transverse interactions dominate the longitudinal ones and the full expression (28) must be used. As we will show below, thermal conductivities, viscosities, and electrical conductivities are also different from those of Haensel and Jerzak.

IV. TRANSPORT COEFFICIENTS

Having evaluated \mathbf{Q}_q and τ_s we proceed to look at various transport processes. We start by calculating the momentum relaxation time of two interpenetrating quark plasmas which follows from the results of the previous section in a straightforward way. Subsequently, we evaluate diffusion coefficients and the electrical conductivity. Finally, we calculate the viscosity and thermal conductivity which require somewhat more elaborate calculations.

A. Momentum relaxation times

Consider a spatially uniform quark plasma of flavor q flowing with respect to $N_q - 1$ plasmas with different flavors ($q' \neq q$). The relative flow velocity will relax in time due to collisions, and we here evaluate the characteristic time for this process. Multiplying (1) by momentum \mathbf{p}_1 and summing we obtain

$$\frac{d\mathbf{g}_q}{dt} = \mathbf{Q}_q, \quad (29)$$

where \mathbf{g}_q is the momentum density

$$\mathbf{g}_q = \nu_q \sum_{\mathbf{p}} \mathbf{p} f_q(\varepsilon_{\mathbf{p}}) = \mathbf{u}_q w_q, \quad (30)$$

and $w_q = \mu_q^4 / \pi^2$ is the enthalpy density for degenerate quark matter of one flavor at $T = 0$. In the center-of-mass system $\mathbf{u}_q = -(N_q - 1)\mathbf{u}_{q'}$ and assuming $\mu_q \simeq \mu_{q'}$ we thus see from (27)–(30) that the momentum density decays exponentially:

$$\mathbf{g}_q(t) = \mathbf{g}_q(0) \exp(-t/\tau_s), \quad (31)$$

with a decay time τ_s . This behavior is strictly true only initially, since scattering drives the plasmas out of local equilibrium so that the later stages will be more complicated. In addition instabilities may appear [15].

The resulting time scale for momentum relaxation is

$$\tau_s \simeq 0.3 \left(\frac{\mu_q}{300 \text{ MeV}} \right)^{2/3} \left(\frac{\alpha_s T}{100 \text{ MeV}} \right)^{-5/3} \text{ fm}/c, \quad (32)$$

for $T \ll q_D \ll \mu_q$ and

$$\tau_s \simeq 0.5 \alpha_s^{-2} \left(\frac{T}{100 \text{ MeV}} \right)^{-1} \ln^{-1}(T/q_D) \text{ fm}/c, \quad (33)$$

for $q_D \ll T \ll \mu_q$. For comparison we give the momentum relaxation times for quarks and gluons in high-temperature plasmas from [5]

$$\tau_s \sim 2 \alpha_s^{-2} \ln^{-1}(1/\alpha_s) \left(\frac{T}{100 \text{ MeV}} \right)^{-1} \text{ fm}/c, \quad (34)$$

In relativistic heavy ion collisions, the central rapidity region is expected to have $T \sim 200 \text{ MeV}$ and $\mu_q \ll T$ and the relaxation times are thus of order a few fm/c for $\alpha_s \sim 0.5$. In the target and projectile fragmentation regions the baryon density may be high and if the excitation energies are low, $T \ll \mu_q \sim 200 \text{ MeV}$, the relaxation times can be longer. For $T \sim \mu_q$ the relaxation times are, however, also of order a few fm/c.

B. Diffusion in burning processes

Transport processes play a major role in the burning of a neutron star into strange quark matter as described in [16]. When a neutron at the phase boundary enters the quark matter, the quarks become deconfined into a u and two d quarks. The d quarks, which are the fuel, have to be transported into the burning region where they are converted to s quarks on a weak-interaction time scale τ_w . The s quarks, which are the waste, have to be transported to the phase boundary or burning front. Thus d and s quarks diffuse through each other and the u quarks; i.e., there are flows of different flavor quarks relative to each other. The burning drives the diffusion which is balanced by friction due to collisions. Since thermal equilibrium is established on strong-interaction time scales, which are very short, whereas burning takes place on longer time scales controlled by weak interactions, we can generally assume the quarks to be in local equilibrium [16] as given by (13) with $T_u = T_s = T_d \equiv T$.

The collision integral on the right side of Eq. (1) consists of a friction term arising from the different quark flavors having different flow velocities. Multiplying the Boltzmann equation (1) by momentum and summing we obtain

$$\nabla_{\mathbf{r}} P_q = \sum_{\mathbf{p}_1} \mathbf{p}_1 \left(\frac{\partial f_q}{\partial t} \right)_{\text{coll}} = \mathbf{Q}_q. \quad (35)$$

Here $P_q = \mu_q^4 / 4\pi^2$ is the pressure from quarks of flavor q . As described in [16] this expression for the pressure gradient together with the rate of s -quark conversion and the boundary conditions describe the burning process.

To estimate the parameters in the burning process we take the characteristic values $T \sim 10 \text{ MeV}$ for the neutron matter temperature and $\sim 300 \text{ MeV}$ for the quark chemical potentials. Taking the perturbative running coupling constant

$$\alpha_s(T) \simeq 6\pi / [(33 - 2N_f) \ln(\mu_q/\Lambda)],$$

with $\Lambda \sim 150$ MeV, we find $\alpha_s \sim 1$ at these densities (so perturbation theory may not be trustworthy). With the value $\alpha_s = 0.5$ in (28) [the maximum value for which $q_D < \mu_q$, as required for the validity of (28)] we obtain

$$\tau_s \simeq 5 \times 10^2 \left(\frac{\mu_q}{300 \text{ MeV}} \right)^{2/3} \left(\frac{T}{10 \text{ MeV}} \right)^{-5/3} \text{ fm}/c;$$

also

$$\tau_w \simeq 10^{15} \left(\frac{\mu_q}{300 \text{ MeV}} \right)^{-3} \left(\frac{T}{10 \text{ MeV}} \right)^{-2} \text{ fm}/c$$

so that $\sqrt{\tau_s/\tau_w}c \sim 100 \text{ m s}^{-1}$. The front velocity will be an order of magnitude smaller, $u_F \sim 10 \text{ m/s}$. A neutron star of radius $\sim 10 \text{ km}$ will thus burn in $\sim 10^3 \text{ s}$. Generally the time scale is set by τ_w and the length scale by $c\sqrt{\tau_s\tau_w}$, so that the scale of the front velocity is set by $c\sqrt{\tau_s/\tau_w}$.

The burning scenario only applies to the burning of bulk nuclear matter into bulk quark matter. As described in [17] the cores of neutron stars may consist of quark matter droplets embedded in the nuclear matter or more complicated rod and platelike structures. Because of Coulomb energies in this two-component system the mixed phase of quark and nuclear matter is energetically the most favorable state; this is similar to the phase in neutron star crusts above neutron drip.

One may define a diffusion coefficient D by the ratio of the flux of quarks of flavor q to the density gradient, $\mathbf{u}_q n_q = -D \nabla_r n_q$, where $n_q = \mu_q^3/\pi^2$ is the q -quark number density. Letting one of the quark components with velocity \mathbf{u}_1 diffuse through the others with velocity \mathbf{u}_2 we have that $\mathbf{u}_2 = -\mathbf{u}_1/(N_q - 1)$ in the center-of-mass system. Consequently, we obtain from (35) and (27) that

$$D = \frac{\tau_s}{3}. \quad (36)$$

The diffusion coefficient is thus of the same order of magnitude as the relaxation time τ_s or the stopping length since all particle speeds are $c = 1$. It has been customary to estimate the mean free path by the inverse of the quark-quark scattering cross section, σ_{qq} , times the quark density and a factor taking Pauli blocking into account: $\lambda \sim (\sigma_{qq} n_0)^{-1} (\mu/T)^2$; usually one estimates the quark scattering cross section by a third of the proton-proton cross section: $\sigma_{qq} \sim \sigma^{pp}/3$. Thus

$$\lambda \simeq 8 \left(\frac{\mu_q}{300 \text{ MeV}} \right)^{-1} \left(\frac{T}{100 \text{ MeV}} \right)^{-2} \text{ fm}.$$

This estimate for λ is independent of α_s and q_D , and has a different temperature dependence than the stopping length $\sim c\tau_s$ because the latter takes the very singular forward scattering into account. Quantitatively, λ is longer than $c\tau_s$ unless a low value for $\alpha_s \simeq 0.15$ is chosen when $T \simeq 100 \text{ MeV}$ and $\mu \simeq 300 \text{ MeV}$.

C. Electrical conduction

For u , d , and s quark matter with $m_s = 0$ there are no electrons present since charge neutrality is automatically satisfied. Thus all electrical currents must be carried by quarks. Applying an electric field \mathbf{E} to the quark plasma will generate an electrical current in which u quarks flow in the direction of the electric field, and d and s quarks flow in the opposite direction. In a steady state friction due to collisions will balance the electric force.

A rigorous calculation of the electrical conductivity requires knowledge of the nonequilibrium quark distribution functions. To determine the deviation from local equilibrium one must take into account the scatterings of the interpenetrating quark plasmas as well as the scatterings within each quark flavor which will equilibrate the distributions functions towards the local equilibrium ones. The quark conductivity can, however, be estimated by assuming that the distribution functions are given as (13) where \mathbf{u}_1 is the flow velocity of u quarks and \mathbf{u}_2 is that of d and s quarks. d and s quarks have the same charge and therefore the same velocity. We assume weak fields so that $\mathbf{u}_i \ll c$ and in the rest frame of all the quarks $\mathbf{u}_1 = -2\mathbf{u}_2$.

In a steady-state, isotropic plasma we obtain, from the Boltzmann equation,

$$e_q \mathbf{v}_1 \cdot \mathbf{E} \left(\frac{\partial f_q^0(\varepsilon_1)}{\partial \varepsilon_1} \right) = \left(\frac{\partial f_q}{\partial t} \right)_{\text{coll}}, \quad (37)$$

where e_q is the electrical charge of a quark, $e_q = \frac{2}{3}e$ for u quarks, and $e_q = -\frac{1}{3}e$ for d and s quarks. Multiplying (37) by \mathbf{p}_1 and summing over momenta $\mathbf{p}_1 = \mathbf{p}$ we find that the RHS gives us exactly \mathbf{Q}_q (as described in Appendix A only particles at the Fermi surface contribute to the scatterings when $T \ll \mu_q$ and so $\mathbf{p} \simeq \mu_q \mathbf{v}_p$). Consequently, we obtain the simple result

$$e_q \mathbf{E} n_q = \mathbf{Q}_q. \quad (38)$$

For u , d , and s quark matter with $m_s \ll \mu_s$, the electrical current is $\mathbf{j}_{\text{el}} = \sum_q e_q \mathbf{u}_q f_q = e \mathbf{u}_1 n_q$. The electrical conductivity is thus, from (38) and (28),

$$\sigma_{\text{el}} = j_{\text{el}}/E = \frac{2}{3} \frac{\mu_q^2}{\pi^2} e^2 \tau_s. \quad (39)$$

This result may be understood simply in terms of the quark electrical conductivity. It actually becomes the standard Drude result for a multicomponent system, $\sigma_{\text{el}} = \sum_q n_q e_q^2 \tau_q / m_q$, when the density of carriers is taken as $n_q = \mu_q^2/\pi^2$, the masses as $m_q = \mu_q$, the charges e_q as $\frac{2}{3}e$ and $\frac{1}{3}e$ for the u and d, s quarks, respectively, and finally the relaxation time τ_q is replaced by the momentum stopping time τ_s .

If neutron stars with temperatures of order 100 keV or $\sim 10^9 \text{ K}$ have cores of quark matter, the electrical conductivity will be

$$\sigma_{el} \simeq (\alpha_s T_9)^{-5/3} \left(\frac{\mu_q}{300 \text{ MeV}} \right)^{8/3} \times 10^{19} s^{-1}, \quad (40)$$

where T_9 is the temperature in 10^9 K. The quark electrical conductivity is a few orders of magnitude less than the electric conductivity expected in ordinary neutron stars due to electrons.

If the strange quark mass m_s is nonzero, charge neutrality requires that electrons be present in the plasma and since they interact only through the weaker electromagnetic interactions they scatter less and they may dominate the current. The density of electrons to ensure charge neutrality is, however, very small. Even for pure u and d quark matter the electron chemical potential will be only about a quarter of the quark chemical potential and the electron density will only be $\sim 2 \times 10^{-3}$ of the quark density. The exact relation between the quark and electron conductivities depends on m_s and α_s . Thermally produced electrons and positrons can be neglected when $T \ll \mu_q$.

D. Viscosity

The standard methods for calculating transport properties of normal Fermi liquids exactly [14] cannot be used for degenerate quark and electron plasmas because of the singular interaction, which means that it is not possible to decouple integrations over angles from those over quasiparticle energies. Consequently, we shall restrict ourselves in this paper to making variational estimates.

Consider a time-independent flow velocity \mathbf{u} which has only an x component which depends only on y . To calculate the viscosity we linearize the Boltzmann equation, writing the distribution function as

$$f_i = f_i^{le} + \frac{\partial f_i^0}{\partial \varepsilon_i} \Phi_i \frac{\partial u_x}{\partial y}, \quad (41)$$

where $f_i^{le} = \{\exp[(\varepsilon_i - \mu - \mathbf{u} \cdot \mathbf{p}_i)/T] + 1\}^{-1}$ is the local equilibrium distribution function. The Boltzmann equation (1) then reduces to

$$p_{1x} v_{1y} \frac{\partial f_1^0}{\partial \varepsilon_1} = \frac{2\pi\nu_q}{T} N_q \sum_{\mathbf{q}, \mathbf{p}_2} \langle |M_{qq'}|^2 \rangle f_1^0 f_2^0 (1 - f_3^0) (1 - f_4^0) \delta(\varepsilon_1 + \varepsilon_2 - \varepsilon_3 - \varepsilon_4) (\Phi_1 + \Phi_2 - \Phi_3 - \Phi_4). \quad (42)$$

The variational expression for the shear viscosity η is [14]

$$\frac{1}{\eta} \geq \left(\nu_q \sum_{\mathbf{p}} p_x v_y \frac{\partial f^0}{\partial \varepsilon_p} \Psi_{\mathbf{p}} \right)^{-2} \frac{\pi}{2T} \sum_{\mathbf{q}, \mathbf{p}_1, \mathbf{p}_2} \langle |M_{qq'}|^2 \rangle f_1^0 f_2^0 (1 - f_3^0) (1 - f_4^0) \delta(\varepsilon_1 + \varepsilon_2 - \varepsilon_3 - \varepsilon_4) (\Psi_1 + \Psi_2 - \Psi_3 - \Psi_4)^2. \quad (43)$$

The maximum of the right-hand side is achieved when $\Psi = \Phi$. We shall not attempt to solve the integral equation (42) for Φ but rather take the standard ansatz for the deviation from local equilibrium which obeys the symmetry

$$\Psi_{\mathbf{p}} \propto p_x v_y. \quad (44)$$

The constant of proportionality is irrelevant as it cancels in (43) and we shall in the following set it to one. Consequently, the momentum flux tensor is

$$\nu_q \sum_{\mathbf{p}} p_x v_y \frac{\partial f^0}{\partial \varepsilon_p} \Psi_{\mathbf{p}} = \frac{\mu_q^4}{5\pi^2}. \quad (45)$$

$$I_\eta(T/q_D) \equiv \int_0^\infty \frac{d\omega}{\omega} \left(\frac{\omega/2T}{\sinh(\omega/2T)} \right)^2 \int_0^1 dx \int_0^{2\pi} \frac{d\phi}{2\pi} (1-x^2)(1-\cos\phi) \times \left| \frac{1}{1+(xq_D/\omega)^2 \chi_t(x)} - \frac{\cos\phi}{1+(xq_D/\omega)^2 \chi_t(x)/(1-x^2)} \right|^2. \quad (48)$$

This function is also shown in Fig. 3 and can be evaluated analytically in the limits

$$I_\eta(T/q_D) = \begin{cases} \frac{5}{3} \ln(T/q_D) + 3.57, & T \gg q_D, \\ a \left(\frac{T}{q_D} \right)^{2/3} + \frac{\pi^3}{4} \frac{T}{q_D}, & T \ll q_D. \end{cases} \quad (49)$$

Since $\langle |M_{qq'}|^2 \rangle$ depends only on the relative orientation of \mathbf{q} , \mathbf{p}_1 , and \mathbf{p}_2 , we can average over x and y directions while keeping x and ϕ fixed. This corresponds to keeping the relative positions of the three vectors \mathbf{q} , \mathbf{p}_1 , and \mathbf{p}_2 fixed and then rotating this system over the three Euler angles. Consequently, we obtain

$$\overline{(\Psi_1 + \Psi_2 - \Psi_3 - \Psi_4)^2} = \frac{2}{5} q^2 (1-x^2) (1-\cos\phi), \quad (46)$$

where the bar denotes an average over the Euler angles. From (43) we obtain, by comparison with (19),

$$\frac{1}{\eta} = 40\pi\alpha_s^2 \mu_q^{-4} T I_\eta(T/q_D), \quad (47)$$

where

This viscous calculation is more complicated than that for the momentum relaxation time because (46) introduces dependences on angles between \mathbf{p}_1 and \mathbf{p}_2 (or equivalently ϕ , see Appendix A) and so the cross term between longitudinal and transverse interactions in the collision term no longer vanishes. Electrical conduction

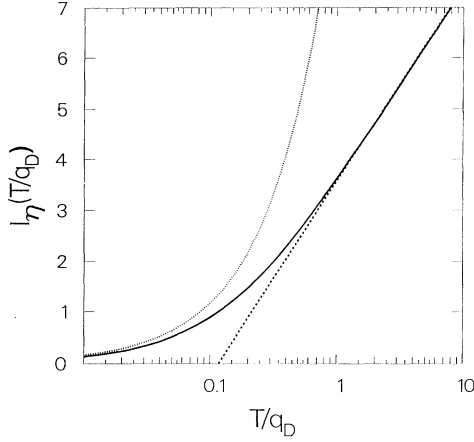


FIG. 3. The dimensionless function $I_\eta(T/q_D)$ given by (48). Dashed and dotted curves correspond to the $T \gg q_D$ and $T \ll q_D$ limits of $I_\eta(T/q_D)$, respectively, as given by (49).

does not introduce such angular dependences which explains why the calculation of the electrical conductivity was simpler. Otherwise, the evaluation is analogous to that for the momentum relaxation time, which is why $I_\eta = I_s$ for transverse interactions alone in the $T \ll q_D$ limit. The cross term contributes to order T/q_D and this term in I_η is therefore three times that in I_s . Because of the extra factor $(1 - \cos \phi)$, the $T \gg q_D$ limit for I_η has a factor $5/2$ instead of the factor $3/2$ in the case of I_s .

The viscous relaxation time is defined by

$$\eta = \frac{1}{5} n p_F v_F \tau_\eta, \quad (50)$$

where $p_F = \mu_q$ is the Fermi momentum, $v_F = c = 1$ is the Fermi velocity and $n = N_q n_q$ is the density of quarks. From (47) we find

$$\begin{aligned} \frac{1}{\tau_\eta} &= \frac{8}{\pi} N_q \alpha_s^2 T I_\eta(T/q_D) \\ &= \frac{8}{\pi} N_q \alpha_s^2 \times \begin{cases} \frac{5}{3} T \ln(T/q_D) + 3.57T, & T \gg q_D, \\ a \frac{T^{5/3}}{q_D^{2/3}} + \frac{\pi^3 T^2}{4 q_D}, & T \ll q_D. \end{cases} \quad (51) \end{aligned}$$

We see that the viscous rate is exactly three times the momentum stopping rate, $1/\tau_s$, of Eq. (28) in the extreme $T \ll q_D$ limit. This is the same ratio as one obtains from standard Fermi liquid theory if small angle scattering processes dominate and the deviation from local equilibrium only depends on q but not on x and ϕ . In our case the transverse interactions dominate for $T \ll q_D$ for which only small x contributes. Furthermore, the $\cos \phi$ term in (46) vanishes since it is an odd power of $\cos \phi$. Therefore the viscous deviation from local equilibrium, Eq. (46), essentially depends only on q . This explains why the viscous rate is just three times $1/\tau_s$. In the $T \gg q_D$ limit, averaging over $1 - x^2$ gives an additional factor $2/3$ and the factor $(1 - \cos \phi)$ in addition to the $(1 - \cos \phi)^2$ factor from the matrix element [see, e.g., Eq. (9)] gives a factor $5/2$ instead of the factor $3/2$ in the calculation of $1/\tau_s$. Consequently, the viscous rate is $1/\tau_\eta = 10/(3\tau_s)$ as can be seen by comparing (51) with (28) in the extreme $T \gg q_D$ limit.

The bulk viscosity for weakly interacting extremely relativistic particles vanishes, just as it does for weakly interacting nonrelativistic particles. The reason for this is that in both cases the particle energy is a homogeneous function of the momentum, and consequently a homologous compression of the system leads to another equilibrium state, but with different temperature and chemical potential [1, 18]. When the strange quark has a finite mass, compression of strange quark matter leads to a state out of β equilibrium. The relaxation of this state by weak interactions gives rise to a bulk viscosity, which Madsen has calculated in detail [19]. Strong interactions, which dominate the behavior of the transport and relaxation process considered in this paper, play only a minor role in the bulk viscosity.

E. Thermal conductivity

To calculate the thermal conductivity we linearize the Boltzmann equation, writing the distribution function as

$$f_i = f_i^{le} + \frac{\partial f_i^0}{\partial \varepsilon_i} \Phi_i \frac{\nabla T}{T}, \quad (52)$$

where $f_i^{le} = \{\exp[(\varepsilon_i - \mu)/T(z)] + 1\}^{-1}$ is the local equilibrium distribution function; one finds

$$v_{1z}(\varepsilon_1 - \mu) \frac{\partial f_1^0}{\partial \varepsilon_1} = \frac{2\pi\nu_q}{T} N_q \sum_{\mathbf{q}, \mathbf{p}_2} f_1^0 f_2^0 (1 - f_3^0)(1 - f_4^0) \langle |M_{qq'}|^2 \rangle \delta(\varepsilon_1 + \varepsilon_2 - \varepsilon_3 - \varepsilon_4) (\Phi_1 + \Phi_2 - \Phi_3 - \Phi_4). \quad (53)$$

The thermal conductivity κ is given by [14] the maximum of

$$\begin{aligned} \frac{1}{\kappa} &\geq \left(\nu_q \sum_{\mathbf{p}} (\varepsilon_{\mathbf{p}} - \mu) v_z \frac{\partial f_{\mathbf{p}}^0}{\partial \varepsilon_{\mathbf{p}}} \Psi_{\mathbf{p}} \right)^{-2} \\ &\times \frac{\pi}{2} \sum_{\mathbf{q}, \mathbf{p}_1, \mathbf{p}_2} \langle |M_{qq'}|^2 \rangle f_1^0 f_2^0 (1 - f_3^0)(1 - f_4^0) \delta(\varepsilon_1 + \varepsilon_2 - \varepsilon_3 - \varepsilon_4) (\Psi_1 + \Psi_2 - \Psi_3 - \Psi_4)^2. \end{aligned} \quad (54)$$

As for the viscosity, we calculate the thermal conductivity by taking the standard ansatz,

$$\Psi_{\mathbf{p}} \propto (\varepsilon_{\mathbf{p}} - \mu) v_z, \quad (55)$$

for currents in the z direction. Consequently, we find for the normalizing factor in (54), essentially the thermal current per quark flavor,

$$J_T = \nu_q \sum_{\mathbf{p}} (\varepsilon_{\mathbf{p}} - \mu_q) v_z \frac{\partial f^0}{\partial \varepsilon_{\mathbf{p}}} \Psi_{\mathbf{p}} = \frac{1}{3} \mu_q^2 T^2. \quad (56)$$

From (54) and (55) we obtain, after averaging over directions of the z axis (i.e., the three Euler angles as before) keeping x and ϕ fixed,

$$(\Psi_1 + \Psi_2 - \Psi_3 - \Psi_4)^2 = \frac{2}{3} \omega^2 (1 - x^2) (1 - \cos \phi), \quad (57)$$

to leading orders in ω and q . Note that in the case of thermal conduction (57) one obtains a factor ω^2 whereas in the case of momentum relaxation and viscous flow we found a factor q^2 [see Eq. (46)]. We find

$$\frac{1}{\kappa} = \frac{24}{\pi^3} \alpha_s^2 T^{-2} I_{\kappa}(T/q_D), \quad (58)$$

where

$$I_{\kappa}(T/q_D) \equiv \int_0^{\infty} \frac{d\omega}{\omega} \left(\frac{\omega/2T}{\sinh(\omega/2T)} \right)^2 \int_0^1 dx \int_0^{2\pi} \frac{d\phi}{2\pi} x^2 (1 - x^2) (1 - \cos \phi) \times \left| \frac{1}{1 + (xq_D/\omega)^2 \chi_t(x)} - \frac{\cos \phi}{1 + (xq_D/\omega)^2 \chi_t(x)/(1 - x^2)} \right|^2. \quad (59)$$

This function can be evaluated analytically in the two limits

$$I_{\kappa}(T/q_D) = \begin{cases} \frac{1}{3} \ln(T/q_D) + 0.30, & T \gg q_D, \\ 2\zeta(3) \left(\frac{T}{q_D} \right)^2, & T \ll q_D. \end{cases} \quad (60)$$

In the $T \ll q_D$ limit we have given only the term coming from purely transverse interactions. The cross term contributes to order $(T/q_D)^{8/3}$ and higher whereas the purely longitudinal interactions contribute to order $(T/q_D)^3$ and higher.

The full result obtained by performing the x and ω integrations numerically is shown in Fig. 4.

We define a characteristic relaxation time for thermal conduction, τ_{κ} , by

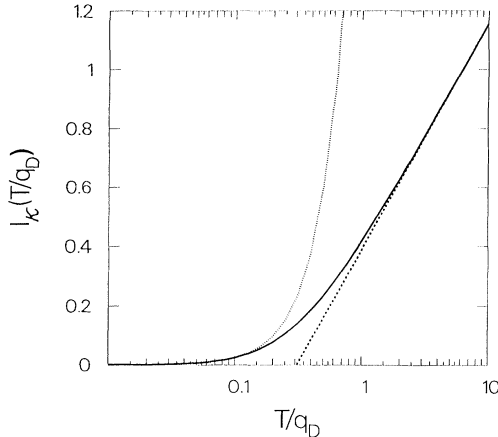


FIG. 4. The dimensionless function $I_{\kappa}(T/q_D)$ given by (59). Dashed and dotted curves correspond to the $T \gg q_D$ and $T \ll q_D$ limits of $I_{\kappa}(T/q_D)$, respectively, as given by (60).

$$\kappa = \frac{1}{3} v_F^2 c_v \tau_{\kappa}, \quad (61)$$

where $c_v = (N_q/2) T \mu_q^2$ is the specific heat per volume. Thus we find

$$\frac{1}{\tau_{\kappa}} = \frac{4}{\pi^3} N_q \alpha_s^2 \frac{\mu_q^2}{T} I_{\kappa}(T/q_D) = \frac{4}{\pi^3} N_q \alpha_s^2 \mu_q^2 \times \begin{cases} \frac{\ln(T/q_D)}{3T} + \frac{0.30}{T}, & T \gg q_D, \\ 2\zeta(3) T/q_D^2, & T \ll q_D. \end{cases} \quad (62)$$

The relaxation time for thermal conduction has a different temperature dependence than both τ_s and τ_{η} because the thermal conduction was weighted by energy transfers (ω^2) instead of momentum transfers (q^2) as for momentum stopping, electrical conduction and viscous processes.

We now discuss how one may understand in simple terms why the temperature dependence of the relaxation rate for thermal conduction differs from those for the other processes we have considered. If one derives expressions for the relaxation rates using the calculations given above, one finds that they all have similar forms, but a weighting factor $\sim (q/p_F)^2$ in the relaxation rates for viscosity, electrical conductivity, and momentum is replaced by a factor $\sim (\omega/T)^2$ in the relaxation rate for thermal conductivity. For the case $T \gg q_D$ the dominant contribution to rates comes from processes with $\omega \sim q \sim T$, and therefore the thermal conduction rate is a factor $\sim (\mu/T)^2$ greater than the other rates. In the opposite limit, $T \ll q_D$, processes with $\omega \sim T$ and $q \sim (q_D^2 T)^{1/3}$ are most important, and consequently the thermal conduction rate is a factor $\mu^2/(T^{2/3} q_D^{4/3})$ larger.

As mentioned above the purely longitudinal interac-

tions gave a $(T/q_D)^3$ contribution to I_κ in limit of $T \ll q_D$. Therefore, for longitudinal processes alone, $1/\tau_\kappa$ has the standard Fermi liquid T^2 dependence just like $1/\tau_s$ and $1/\tau_\eta$ as explained above in connection with the calculation of $1/\tau_s$.

V. SUMMARY

Our calculations above show that the transport properties of degenerate QCD or QED plasmas of relativistic particles have several interesting features. First, there are three scales, the chemical potentials, the temperature, and the Debye screening wave number. We have investigated the degenerate case where μ is much larger than T and q_D and found that the physics changes between the two limiting cases of $T \gg q_D$ and $T \ll q_D$. Second, we found that the transverse interactions dominate the scattering processes when $T \ll q_D$ because they are only screened for energy transfers less than $\sim (q_D^2 T)^{1/3}$. The resulting relaxation rates for momentum relaxation, electrical conduction, and viscous processes scale as $1/\tau \sim (\alpha_s T)^{5/3}/\mu_q^{2/3}$, while the relaxation rate for thermal conduction is $1/\tau_\kappa \sim \alpha_s T$. The qualitative reason for τ_κ behaving in a different way from the other relaxation times is related to the singular character of the interaction for small energy transfer and small momentum transfer.

At high temperatures, $T \gg q_D$, relaxation times are similar to those of hot nondegenerate quark-gluon plasmas where the rates of momentum relaxation are $1/\tau_s \sim T\alpha_s^2 \ln(T/q_D)$. However, the Debye wave number is different, $q_D \sim gT$. At low temperatures, $T \ll q_D$, the result is qualitatively different from that as well as from standard Fermi liquids [14]. The relation $1/\tau_s \sim \alpha_s^2 T^{5/3}/q_D^{2/3}$ was found instead because the energy transfers are limited by the temperature and not the Debye wave number when $T \ll q_D$. Whereas dynamical screening drastically influences the transport coefficients for degenerate quark matter it only enters through the factor $\ln(T/q_D)$ in high-temperature plasmas. If a magnetic mass $m_{\text{mag}} \sim g^2 T$ were responsible for the infrared cutoff instead of q_D in dynamical screening, the only difference would be a factor of 2 in the leading logarithmic order. The results obtained here are exact to order α_s^2 whereas previous results for $T \gg \mu_q$ were limited to leading logarithmic order, $\alpha_s^2 \ln(1/\alpha_s)$.

The viscosity was found to be similarly influenced by

dynamical screening and can be written as $\eta \simeq w_q \tau_s/5$ where the viscous relaxation time is, from (47), approximately one-third of the momentum relaxation time. The thermal conductivity, however, has a different behavior for $T \ll q_D$ as seen in (58) because the thermal transport is reduced as compared to transport of momentum. An important general conclusion of these studies of QCD and QED plasmas is that the relaxations times are different for different transport processes and all deviate from the standard results of Fermi liquid theory.

ACKNOWLEDGMENTS

This work was supported in part by U.S. National Science Foundation Grants No. PHY89-21025 and No. PHY91-00283, NASA Grant No. NAGW-1583, DOE Grant No. DE-AC03-76SF00098, and the Danish Natural Science Research Council. Discussions with Gordon Baym and Geoff Ravenhall are gratefully acknowledged.

APPENDIX A: THE STRUCTURE FACTOR

Here we evaluate the structure function of Eq. (18). We introduce auxiliary integrals over the momentum and energy transfers so that

$$\delta(\mathbf{p}_1 + \mathbf{p}_2 - \mathbf{p}_3 - \mathbf{p}_4) = \int d^3 \mathbf{q} \delta(\mathbf{p}_1 - \mathbf{p}_3 - \mathbf{q}) \times \delta(\mathbf{p}_2 - \mathbf{p}_4 + \mathbf{q}), \quad (\text{A1})$$

$$\delta(\varepsilon_1 + \varepsilon_2 - \varepsilon_3 - \varepsilon_4) = \int d\omega \delta(\varepsilon_1 - \varepsilon_3 - \omega) \times \delta(\varepsilon_2 - \varepsilon_4 + \omega), \quad (\text{A2})$$

whereby the sums over 1 and 3 separates the sums over 2 and 4 in (12).

The three-dimensional δ function expressed in spherical coordinates is

$$\delta(\mathbf{p}_1 - \mathbf{p}_3 - \mathbf{q}) = \frac{2}{p_3} \delta(p_3^2 - (\mathbf{p}_1 - \mathbf{q})^2) \times \delta(\cos \theta_3 - \cos \theta_{1q}) \delta(\phi_3 - \phi_{1q}), \quad (\text{A3})$$

where θ_3 and θ_{1q} are the polar angles of the vectors \mathbf{p}_3 and $\mathbf{p}_1 - \mathbf{q}$, respectively, and ϕ_3 and ϕ_{1q} are the corresponding azimuthal angles. Since we already have linearized in the flow velocities they can be set to zero in distribution functions in (17). From (17) and (A3) we obtain

$$\begin{aligned} S(\mu_q, q, \omega) &= 2(2\pi)^{-5} \int_\omega^\infty dp_1 f_q^0(p_1) [1 - f_q^0(p_1 - \omega)] p_1 (p_1 - \omega) \int_{-1}^1 d \cos \theta \delta(\omega^2 - 2p_1 \omega - q^2 + 2p_1 q \cos \theta) \\ &= (2\pi)^{-5} \frac{\Theta(q - |\omega|)}{q} \int_{(q+\omega)/2}^\infty dp_1 f_q^0(p_1) [1 - f_q^0(p_1 - \omega)] p_1 (p_1 - \omega). \end{aligned} \quad (\text{A4})$$

Here θ is the angle between \mathbf{p}_1 and \mathbf{q} which, due to the δ function, is limited to $\cos \theta = \omega/q = x$. Since the matrix element depends on $\cos \phi$ where $\phi = \phi_{2q} - \phi_{1q}$, we must transform the variables ϕ_{1q} and ϕ_{2q} to ϕ and, for example, ϕ_{1q} . In (A4) the integration over ϕ_{1q} has been performed giving 2π . Consequently, we are left with an average $\langle |M|^2 \rangle_\phi = \int_0^{2\pi} d\phi/2\pi |M|^2$, which must be performed in the integrals of Eq. (16) in order to obtain Eq. (19).

Since $\omega \lesssim T \ll \mu_q$ the lower limit of the integral can be approximated by $q/2$ and we get

$$S(\mu_q, q, \omega) \simeq (2\pi)^{-5} \frac{\Theta(q - |\omega|)}{q} \mu_q^2 \Theta(2\mu_q - q) \frac{\omega}{\exp(\omega/T) - 1}, \quad (\text{A5})$$

which contains the usual Bose factor for the transferred gluon of energy $-\omega$.

The upper cutoff on the momentum transfer, $q \leq 2\mu_q$, will actually not enter in the calculations because the energy transfer is limited by the temperature and we are considering the limit of $T \ll \mu_q$. The condition $|\omega| \leq q$ ensures that the gluon transfer occurs in the Landau damping regime.

APPENDIX B: EVALUATION OF $I_s(T/q_D)$

We evaluate the integral over ω and q in (16) in more detail to find the leading logarithmic term as well as the next order in the limit of $q_D \ll T$.

It is convenient to insert an intermediate cutoff, $q_D \ll \tilde{\omega} \ll T$, in the integral of ω so that

$$I_s(T/q_D) = \left[\int_0^{\tilde{\omega}} + \int_{\tilde{\omega}}^{\infty} \right] \frac{d\omega}{\omega} \left(\frac{\omega/2T}{\sinh(\omega/2T)} \right)^2 \int_0^1 dx \left[\frac{1}{|1 + (xq_D/\omega)^2 \chi_l(x)|^2} + \frac{1}{2} \frac{1}{|1 + (xq_D/\omega)^2 \chi_t(x)/(1-x^2)|^2} \right]. \quad (\text{B1})$$

In the second (upper) integral where $q_D \ll \tilde{\omega} \leq \omega$ we can neglect effects of screening so that

$$I^{(u)} = \int_{\tilde{\omega}}^{\infty} \frac{d\omega}{\omega} \left(\frac{\omega/2T}{\sinh(\omega/2T)} \right)^2 \frac{3}{2} = \frac{3}{2} \left[\frac{\tilde{\omega}}{2T} \coth\left(\frac{\tilde{\omega}}{2T}\right) - \ln \sinh\left(\frac{\tilde{\omega}}{2T}\right) - \ln 2 \right] \simeq \frac{3}{2} \left[\ln\left(\frac{T}{\tilde{\omega}}\right) + 1 \right], \quad \tilde{\omega} \ll T. \quad (\text{B2})$$

In the first (lower) integral we can ignore the Bose factors since $\omega \leq \tilde{\omega} \ll T$. To leading logarithmic order the x dependence of χ is unimportant. The integrals over x just give 3/2 with, however, a cutoff when $\omega \lesssim q_D$. Consequently, $I_s = \frac{3}{2} \ln(\tilde{\omega}/q_D)$, to leading order. The next order cannot be performed analytically because of the complicated functions $\chi_{l,t}(x)$. However, when $\omega \gg q_D$ the screening can be ignored and when $\omega \ll q_D$ only the small x behavior of $\Pi_{l,t}$ matters. Therefore we approximate $\chi_{l,t}$ for small arguments (8) and obtain the estimate

$$I^{(l)} \simeq \int_0^{\tilde{\omega}} \frac{d\omega}{\omega} \int_0^1 dx \left[\frac{1}{[1 + (xq_D/\omega)^2]^2} + \frac{1}{2} \frac{1}{|1 + i\pi x^3 q_D^2/(4\omega^2)|^2} \right] \\ \simeq \ln\left(\frac{\tilde{\omega}}{q_D}\right) + \frac{1}{2} + \frac{1}{2} \left[\ln\left(\frac{2\tilde{\omega}}{\sqrt{\pi}q_D}\right) + \frac{3}{2} \right], \quad q_D \ll \tilde{\omega}. \quad (\text{B3})$$

Adding (B2) and (B3) we obtain

$$I_s(T/q_D) \simeq \frac{3}{2} \ln\left(\frac{T}{q_D}\right) + \frac{11}{4} + \frac{1}{2} \ln\left(\frac{2}{\sqrt{\pi}}\right) \\ \simeq \frac{3}{2} \ln\left(\frac{T}{q_D}\right) + 2.810, \quad q_D \ll T. \quad (\text{B4})$$

The constant found in this approximation is remarkably close to the value 2.72 found by numerical integration of (B1). The reason is that the small x expansion exhausts most of the deviation and the corrections from the detailed forms of χ_l and χ_t , as compared to their small x limits, cancel partially by accident.

-
- [1] S. Gavin, Nucl. Phys. **B435**, 826 (1984).
 [2] A. Hosoya and K. Kajantie, Nucl. Phys. **B250**, 666 (1984).
 [3] P. Danielewicz and M. Gyulassy, Phys. Rev. D **31**, 53 (1985).
 [4] G. Baym, H. Monien, and C. J. Pethick, in *Proceedings of the XVI International Workshop on Gross Properties of Nuclei and Nuclear Excitations*, Hirschegg, Austria, 1988, edited by H. Feldmeier (GSI and Institut für Kernphysik, Darmstadt, West Germany, 1988), p. 128; C. J. Pethick, G. Baym, and H. Monien, in *Quark Matter*

- '88, Proceedings of the Seventh International Conference on Ultrarelativistic Nucleus-Nucleus Collisions, Lenox, Massachusetts, 1988, edited by G. Baym, P. Braun-Munzinger, and S. Nagamiya [Nucl. Phys. **A498**, 313c (1989)]; G. Baym, H. Monien, C. J. Pethick, and D. G. Ravenhall, Phys. Rev. Lett. **64**, 1867 (1990).
 [5] G. Baym, H. Monien, C. J. Pethick, and D. G. Ravenhall, in *Quark Matter '90*, Proceedings of the Eighth International Conference on Ultrarelativistic Nucleus-Nucleus Collisions, Menton, France, 1990, edited by J. P. Blaizot *et al.* [Nucl. Phys. **A525**, 415c (1991)]; G. Baym, H.

- Heiselberg, C. J. Pethick, and J. Popp, in *Quark Matter '91*, Proceedings of the Ninth International Conference on Ultrarelativistic Nucleus-Nucleus Collisions, Gatlinburg, Tennessee, edited by T. C. Awes *et al.* [*ibid.* **A544**, 569c (1992)]; and (unpublished).
- [6] G. E. H. Reuter and E. H. Sondheimer, *Proc. R. Soc. A* **195**, 336 (1948).
- [7] P. Haensel and A. J. Jerzak, *Acta. Phys. Pol. B* **20**, 141 (1989); P. Haensel, in *Strange Quark Matter in Physics and Astrophysics*, Proceedings of the International Workshop, Aarhus, Denmark, 1991, edited by J. Madsen and P. Haensel [*Nucl. Phys. B (Proc. Suppl.)* **24B**, 144 (1991)].
- [8] G. Baym and S. Chin, *Nucl. Phys.* **A262**, 527 (1976).
- [9] B. L. Combridge, J. Kripfganz, and J. Ranft, *Phys. Lett.* **70B**, 234 (1977).
- [10] H. A. Weldon, *Phys. Rev. D* **26**, 1394 (1982).
- [11] M. B. Kislinger and P. D. Morley, *Phys. Rep.* **51**, 63 (1979); O. K. Kalashnikov, *Fortschr. Phys.* **32**, 525 (1984).
- [12] T. Holstein, R. E. Norton, and P. Pincus, *Phys. Rev. B* **8**, 2649 (1973).
- [13] M. Yu. Reizer, *Phys. Rev. B* **39**, 1602 (1989); P. A. Lee, *Phys. Rev. Lett.* **63**, 680 (1989).
- [14] G. Baym and C. J. Pethick, *Landau Fermi-Liquid Theory: Concepts and Applications* (Wiley, New York, 1991).
- [15] E. M. Lifshitz and L. P. Pitaevskii, *Physical Kinetics* (Pergamon, New York, 1981), Sec. 61.
- [16] H. Heiselberg, G. Baym, and C. J. Pethick, in *Strange Quark Matter in Physics and Astrophysics* [7], p. 144.
- [17] H. Heiselberg, C. J. Pethick, and E. F. Staubo, *Phys. Rev. Lett.* **70**, 1355 (1993); N. Glendenning, *Phys. Rev. D* **46**, 1279 (1992).
- [18] H. Heiselberg, C. J. Pethick, and D. G. Ravenhall, *Ann. Phys. (N.Y.)* **223**, 23 (1993).
- [19] J. Madsen, *Phys. Rev. D* **46**, 3290 (1992).